Nanoscale

Accepted Manuscript

This is an *Accepted Manuscript*, which has been through the Royal Society of Chemistry peer review process and has been accepted for publication.

Accepted Manuscripts are published online shortly after acceptance, before technical editing, formatting and proof reading. Using this free service, authors can make their results available to the community, in citable form, before we publish the edited article. We will replace this *Accepted Manuscript* with the edited and formatted *Advance Article* as soon as it is available.

You can find more information about *Accepted Manuscripts* in the **Information for Authors**.

Please note that technical editing may introduce minor changes to the text and/or graphics, which may alter content. The journal's standard **Terms & Conditions** and the **Ethical guidelines** still apply. In no event shall the Royal Society of Chemistry be held responsible for any errors or omissions in this *Accepted Manuscript* or any consequences arising from the use of any information it contains.

www.rsc.org/nanoscale

Nanoscale

ARTICLE

Gadolinium oxide nanoplates with high longitudinal relaxivity for magnetic resonance imaging

Minjung Cho[a,b], Richa Sethi[b], Jeyarama Subramanian Ananta narayanan[b],Seung Soo Lee[a], Denise N. Benoit[a], Nasim Taheri[a], Paolo Decuzzi[b,c], Vicki L. Colvin[a*]

Molecular-based contrast agents for Magnetic Resonance Imaging (MRI) are often characterized by insufficient relaxivity, thus requiring the systemic injection of high doses to induce sufficient contrast enhancement at the target site. In this work, gadolinium oxide (Gd_2O_3) nanoplates are produced via a thermal decomposition method. The nanoplates have a core diameter varying from 2 to 22 nm, a thickness of 1 to 2 nm, and are coated with either an oleic acid bilayer or an octylamine modified poly (acrylic acid) (PAA-OA) polymer layer. For the smaller nanoplates, longitudinal relaxivities r_1 of 7.96 and 47.2 $(mM·s)^{-1}$ were measured at 1.41T for the oleic acid bilayer and PAA-OA coating, respectively. These values moderately reduce as the size of the Gd_2O_3 nanoplates increases, and are always larger for the PAA-OA coating. Cytotoxicity studies on human dermal fibroblast document no significant toxicity, with 100% cell viability preserved up to 250 μM for the PAA-OA coated Gd_2O_3 nanoplates. Given the 10 times increase in longitudinal relaxivity over the commercially available Gd-based molecular agents and the favorable toxicity profile, the 2 nm PAA-OA coated Gd_2O_3 nanoplates could represent a new class of highly effective T_1 MRI contrast agents.

Introduction

Magnetic Resonance Imaging (MRI) has emerged as a powerful non-invasive imaging technique because it allows *in vivo* examination of biological samples with excellent spatial resolution.[1-3, 4, 5] They work by either shortening the longitudinal relaxation time (T_1) or the transverse relaxation time (T_2) of water protons. Two contrast agents in use clinically are gadolinium (Gd)-based chelates and iron oxide nanoparticles.[4, 6-12] Gadolinium chelate MR contrast agents are positive contrast agents because they shorten T_1 relaxation time leading to increase signal intensity. Gadolinium-diethylenetriaminepentaacetate (Gd-DTPA, Magnevist[®]) is among the most popular clinical agent; it can be used to enhance tissue pathology, detect leaks in the blood-brain barrier (BBB), and in some cases identify physiological changes in tissue.[7]

There are no commercially available, nanoscale T_1 contrast agents, analogs of the T_2 iron oxide nanoparticles. However a nanoscale reformulation of T_1 contrast agents could offer several unique advantages for biomedical imaging in that nanoparticles can concentrate a large number of magnetic ions in a small volume thus offering a high signal to noise ratio.[11, 13,14] Furthermore, as compared to molecular T_1 agent, nanoparticles can have longer circulation life in the blood, more cellular retention, and various targeting moieties can be readily conjugated on their surfaces to enable molecular imaging. Indeed, an ongoing limitation of Gd-chelates is their toxicity at higher doses and the possible occurrence of nephrologenic system fibrosis (NSF).[15-19] Nanoscale T_1 agents would have a different set of toxicity issues and because of its crystalline form would likely leach less gadolinium as compare to chelates. Given this potential, there has been recent interest in producing gadolinium containing nanoparticles for use as T_1 contrast agents. In particular, gadolinium oxide nanoparticles formed via a low temperature strategy have r_1 relaxivity values up to 10 $(mM·s)^{-1}$, which is comparable to commercial chelates.[20-23] To compete with the clinically approved contrast agents, nanoscale T_1 contrast agents must present substantially higher relaxivities and improved safety profiles. Only recently, ultra-small gadolinium oxide nanoparticles were proposed as *in-vivo* T_1 contrast agents with r_1 relaxivity values ranging between 8 and 15 $(mM·s)^{-1}$.[21, 24-28] A still outstanding question is the extent to which these values can be boosted by controlling the diameter and surface coating of the nanoparticles. Since, water protons must come into close contact with the Gd^{3+}-ions, a proper design of the surface of the gadolinium oxide nanoparticles is critical. In this work, we synthesize gadolinium oxide nanoparticles via a thermal decomposition method. After a physico-chemical characterization of the nanoparticles, the effect on the longitudinal relaxivity r_1 of their characteristic size and surface coating is systematically investigated.

Experimental Section

Chemicals. The Gadolinium nitrate hexahydrate ($Gd(NO_3)_3 \cdot 6H_2O$, 99.99 %), oleic acid (OLAC, technical grade 90 %), oleylamine (OLAM, technical grade 70 %), 1-octadecene (1-ODE, technical grade 90 %), poly(acrylic acid) (PAA, Mw=1800), octylamine (OA, 99 %), dulbecco's modified eagle's medium (DMEM), fetal bovine serum (FBS), penicilin-streptomycin (PS), and trypsin-EDTA were purchased from Sigma-Aldrich. The synthesis was under high purity nitrogen (N_2, 99.99 %) flow. Methanol (99.8 %), acetone (99.5 %), hexane (98.5 %), sodium bicarbonate (99.7 %), and dimethylformamide (DMF, 99.8 %), nitric acid (HNO_3, 70 %) and hydrogen peroxide (H_2O_2, 30 %) were purchased from Fisher Scientific; 1-ethyl-3-[3-dimethylaminopropyl] carboiimide hydrochloride (EDC) was purchased from Thermo Scientific; The CellTiter 96® Aqueous One solution Cell Proliferation Assay (MTS assay) was purchase from Promega; Human derman fibroblast (HDF) cells were purchased from Cambrex.

Synthesis of gadolinium oxide (Gd_2O_3) nanoparticles. 2 mmol of gadolinium nitrate hexahydrate was mixed with oleic acid (4 mmol) and 1-octadecene (5 g) and stirred for 2 hours at 110 ºC until the Gd precursor was completely dissolved in the solvent as Gd-oleate precursors. After increasing the temperature from 110 to 290 ºC, the reaction mixture was refluxed at 290 ºC for 3-18 hours. After the reaction is done, the temperature was cooled down to room temperature. The resulting colloidal solution (5 mL) was centrifuged with methanol (20 mL) and acetone (20 mL) at 4150 rpm for 30 minutes and redispersed with hexane. This purification was repeated six times resulting in purified gadolinium oxide nanoparticle solution. Finally, the Gd_2O_3 nanoparticles (5 nm) were prepared and stored in hexane. To make larger Gd_2O_3 nanoparticles (8, 11, 13, and 22 nm), the oleylamine (2, 6, 8, and 12 mmol) and more 3 g 1-octadecene were added into the gadolinium-oleate mixture (2 mmol gadolinium nitrate hexahydrate, 4 mmol oleic acid, 5 g 1-octadecene) after heating at 110 ºC for 2 hours and then refluxed at 290 ºC for 3-18 hours. For making smaller 2 nm Gd_2O_3 nanoparticles, the refluxed reaction temperature was increased from 290 to 320 ºC with the amounts of gadolinium nitrate hexahydrate (2 mmol), oleic acid (4 mmol), and 1-octadecene (5 g).

Oleic acid bilayer coated Gd_2O_3 nanoparticles. The oleic acid bilayer coated Gd_2O_3 nanoparticles were modified by a previously published procedure.[29] A specific amount of oleic acid (from 30 μL to 300 μL) was introduced to 1 mL of Gd_2O_3 nanoparticles solution dispersed in ethyl ether (1,500 - 4,000 mg/L of Gd ion concentration). After stirring for 24 hours, ultra pure water (Milipore, 18.2 MΩ·cm) or 0.1 M sodium bicarbonate (pH 9) solution was introduced and stirred for 2 hours. Then a probe sonicator (UP 50H, Dr. Hielscher) was used with 60% amplitude for 10 minutes for the dispersion in water. The Gd_2O_3 aqueous solution was further stirred for 1 day to evaporate ethyl ether completely by opening the cap. The purification of water-soluble Gd_2O_3 nanoparticles was carried out using ultracentrifugation (optima L-90K ultracentrifuge, Beckman coulter) at 40,000 rpm for 3 hours twice and followed by syringe filtration (pore size of 0.45 *u*M, Whatman NYL). The resulting clear brown aqueous solution was acquired after purification. To calculate the transfer yield of oleic acid coating, the concentrations of gadolinium ion were compared in both original and transferred solution. Finally, Gd_2O_3 nanoparticles were dispersed in ultra pure water.

Octylamine (OA) modified poly acrylic acid (PAA) (PAA-OA) polymer synthesis. The preparation of PAA-OA polymer and PAA-OA coated Gd_2O_3 nanoparticles followed a previously published procedure.[30] To make PAA-OA copolymer, first PAA (0.6 g, 0.33 mmol) was dissolved in DMF (10 g). After stirring for 10 minutes, EDC (0.58 g, 3 mmol) was added to the PAA/DMF solution, and octylamine (0.5 mL, 3 mmol) was sequentially introduced to the PAA/EDC/DMF solution. After stirring overnight, rotavap was used to remove DMF and keep the PAA-OA solution in a vacuum. The final PAA-OA solution (15 mg/mL) was redispersed in chloroform (40 mL).

PAA-OA coated Gd_2O_3 nanoparticles. The varied amounts of PAA-OA polymer from 1 to 7 mL were mixed with 1mL Gd_2O_3 nanoparticle/chloroform solution (typically 1,500 to 4,000 mg/L of Gd ion concentration). The mixed solution was stirred for 24 hours and then evaporated the chloroform by using vacuum or air. After adding 0.05 M sodium bicarbonate solution (10 mL), a probe sonicator with 60 % amplitude was used for 10 minutes. The resulting solution was purified with ultracentrifugation (40,000 rpm for 3 hours, twice) and filtered out with syringe filter (0.45 uM, Whatman NYL). The clear brown Gd_2O_3 nanoparticle solution was acquired and completely dissolved in ultrapure MQ water.

Cell Culture. Human derman fibroblast (HDF) were used and cultured in Dulbecco's Modified Eagle's Medium (DMEM) with 10% fetal bovine serum (FBS) and 1 % penicilin-streptomycin (PS). The cells were lifted by trypsin-EDTA and re-suspended in media (DMEM with 10% FBS and 1% PS) solution for the passaging.

Cell Viability test (MTS assay). To determine the cell toxicity depending on the surface coatings (oleic acid and PAA-OA), the standard colorimetric assay, MTS (CellTiter 96, Promega) was used. HDF cells were placed and grown in 96 well culture plates with over 80 % confluency. Each set was prepared with different concentration of Gd_2O_3 nanoparticle solutions (0-500 uM). One set was treated as a blank (no nanoparticles) and last set was used for the untreated control (ethanol). The treated cells with Gd_2O_3 nanoparticle aqueous solution were incubated for 24 hours. The solution was then suctioned out and replaced with 100 uL fresh media (DMEM with FBS 10 % and 1 % PS) solution and 20 uL MTS agent to each well. After incubating for 1 hour at 37 °C and 5 % CO_2, the absorbance at 490 nm of the solution was measured with a plate reader (SPectraMax, M2, Molecular devices). The experiment was repeated three times for the average. The LD_{50}, which gives the lethal dose required for half of the cells to die, was calculated by the percentage of the cell viability.

Characterization

Transmission Electron Microscope (TEM). To measure the diameter of the Gd_2O_3 nanoparticles a JEOL 2100 field emission TEM operating at 200 kV with a single tilt holder was used. TEM sample was prepared by evaporation of one drop of Gd_2O_3 nanoparticle solution on the ultrathin 400 mesh copper grids (Ted Pella Inc.). The size and size histograms of Gd_2O_3 nanoparticles were calculated by counting over 1000 particles with Image-Pro Plus 5.0 (Media Cybernetics, Inc., Silver Spring, MD).

X-ray Diffraction (XRD). X-ray powder diffraction of Gd_2O_3 nanoparticles was carried out using a Rigaku D/Max Ultima II with a zero background sample holder. The X-rays were generated at 40 KV and 40 mA and the range of 2θ was 10 to 80 degrees. For the reference the JCPDS card was used.

X-ray Photoelectron Spectroscopy (XPS). XPS data was recorded by PHI quantera with a monochromatic aluminium 38.6 W. An x-ray source, with an x-ray spot size (200 um) with a pass energy of 26 eV was used for the measurement

Dynamic Light Scattering (DLS) and Zeta potential. The hydrodynamic size (nm) and zeta potential (mV) of oleic acid and PAA-OA coated Gd_2O_3 nanoparticles were measured by Malvern Zetasizer Nanoseries (Malvern, UK). The measurement was repeated five times for the average.

Inductive Coupled Plasma-Optical Emission Spectroscopy (ICP-OES). To measure the gadolinium concentration in a nanoparticle, Perkin Elmer ICP-OES equipped with auto sampler was used. The preparation of sample for ICP-OES was prepared by acid digestion using nitric acid (HNO_3 70 %) and hydrogen peroxide (H_2O_2, 30 %).

Total organic carbon (TOC) analyzer. A Shimadzu TOC-L was used to measure the carbon concentration for surface functionalized gadolinium nanoparticles in water. Three replicates of each sample were prepared by adding 1 ml of the stock nanoparticle sample and diluting to 8.5 mL with Milli-Q 18 MΩ pure water. Each sample was run on a total non-purgeable organic carbon (NPOC) assay with triplicate 50 μL injections. The calibrations from 0.5 to 60 ppm were prepared using TOC standard solution (Sigma-Adrich) with high R_2 (0.998) value.

Calculation of grafting density (GD). The calculation of grafting density (σ) was calculated from TOC data using the equation below, similar to previously published method.[31]

$$\sigma = \frac{[C] * MW_n}{MW_p * C_n * [NP] * (4\pi r_{core}^2)}$$

The non-purgeable organic carbon concentration ([C]) from TOC analysis must be converted from mg/L (ppm) to mol/liter (molarity) by considering molar mass of carbon (12,010 mg/mol). To determine the number of polymer molecules the carbon concentration is multiplied by the molecular weight of the monomer (MW_n) and divided by the polymer molecular weight (MW_p) times the number of carbons per monomer (C_n). By dividing the molar concentration of nanoparticles [NP], and the surface area of the particle the resulting grafting density is achieved.

MR Relaxivity measurement. Various concentration of Gd_2O_3 (0.01 – 2 mM) was prepared by dilution from the stock solution of Gd_2O_3 nanoparticles capped with oleic acid and PAA-OA for MR relaxivity measurement. To measure r_1 and r_2 of Gd_2O_3 nanoparticles, the MR relaxometer (NMR analyzer, mq 60, Bruker) at 1.41T was used. The r_1 and r_2 values were calculated by determining the slope of $1/T_1$ or $1/T_2$ (s^{-1}) at varying TR and TE values against gadolinium concentration (mM).

MR phantom imaging. To image phantoms in MR, a MRI clinical 3T Philips Ingenia MRI scanner (Andover, MA, USA) was used. T_1 weighted contrast enhancement was performed running a standard spin-echo (SE) sequence with 500 ms TR and 23 ms TE. The voxel size is 0.4 X 0.4 mm and slice thickness was 1 mm. For this measurement, the different concentrations of Gd_2O_3 aqueous solution (oleic acid, PAA-OA) were used and compared the contrast with Magnevist® (Gd-DTPA) at same concentration.

Results and discussion

Synthesis and physico-chemical characterization of Gd_2O_3 nanoplates

A central goal of this work is to examine the effect of the diameter and surface coating of Gd_2O_3 nanoparticles on the longitudinal r_1 relaxivity in aqueous suspensions. Towards that end, we adapted synthetic methods, generally used to form uniform metal oxide nanocrystals in organic solutions, to the synthesis of gadolinium oxide. This synthesis proceeds via the thermal decomposition of gadolinium nitrate precursors in the presence of organic surfactants (oleic acid or a mixture of oleic acid and oleylamine). Decomposition occurs at high temperature (290 °C) (**Scheme. 1**).
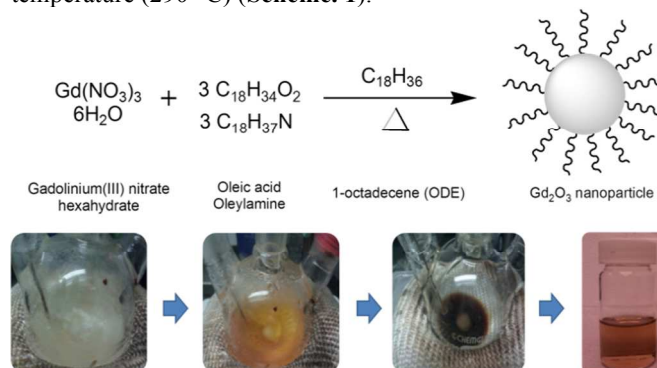
Scheme. 1 Schematic diagram and photographs showing the synthesis of Gd_2O_3 nanoparticles based on thermo-decomposition of gadolinium(III) nitrate hexahydrate in the presence of organic surfactant (oleic acid and oleylamine) and 1-octadecene.

In a typical reaction, a Gd-oleate precursor is firstly prepared by heating gadolinium nitrate hexahydrate and oleic acid at 110°C for two to three hours. This pre-treatment leads to much better particle uniformity than reported before, perhaps because of the ordering of the fatty acid chains.[32] This treatment results in a black-brownish Gd-oleate complex, which is then refluxed at 290 °C under N_2 for three to eighteen hours. The resulting Gd_2O_3 nanoparticles are nearly monodisperse with narrow diameter distributions (<15%) (**Fig. 1**, **Fig. S1, and Fig. S2**). Following this approach, Gd_2O_3 nanoparticles with various diameters were formed, ranging from 2 to 22 nm, by tailoring the reflux time, temperature, precursor concentration, and surfactant type and amount (**Fig. S3**). In **Fig. 1**, transmission electron microscopy (TEM) images are shown for Gd_2O_3 nanoparticles with different core diameters.

The shape, morphology, crystal structure, and composition of Gd_2O_3 nanoparticles were evaluated by transmission electron microscopy (TEM), X-ray photoelectron spectroscopy (XPS), and X-ray diffraction (XRD), respectively. In the TEM images of **Fig. 1**, the some Gd_2O_3 nanoparticles appear as ultrathin plates laying down on the underlying carbon coated copper grid while others are standing on their side perpendicularly to the grid (**Fig. 1 and Fig. S2**). For the standing Gd_2O_3 nanoparticles, an edge thickness of the order of 1.1 to 1.2 nm was measured. Due to high oxophilicity, the oleic acid ligand was strongly bound to the gadolinium nanoparticles rather than oleylamine.[33] The capped oleic acid ligand prevented self-aggregation of nanoparticles via inter-particle dipolar-dipolar repulsive force with good dispersibility (side to side).[34] The size of the Gd_2O_3 nanoparticles was increased by increasing the amount of oleylamine with oleic acid (**Fig. S3**). Note that over the last few years, other authors have also observed that gadolinium oxide and rare earth doped Gd_2O_3 nanoparticles often form unusual

shapes, including nanorings, nanoplates, and ultra-narrow nanorods.[35-39]
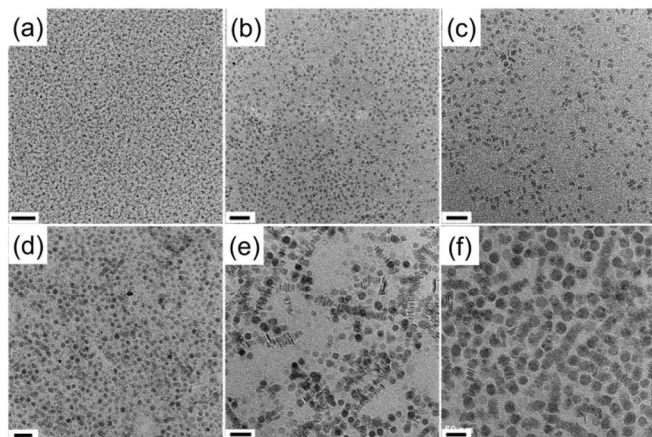
Fig. 1 TEM images of Gd_2O_3 nanoparticles ranging from 2 nm to 22 nm. The diameter of Gd_2O_3 nanoparticles ((a)-(f)) are 1.79 ± 0.23, 5.02 ± 0.45, 7.95 ± 0.82, 10.82 ± 1.75, 13.18 ± 2.09, and 21.97 ± 2.78 nm, respectively. The scale bars are 50 nm except for A (20 nm). The histograms for the size distribution of Gd_2O_3 nanoparticles are shown in supporting information **Fig. S1**.

The chemical composition and crystalline structure of the products were consistent with Gd_2O_3 nanoparticles. XPS found Gd $4d_{3/2}$ and Gd $4d_{5/2}$ features which correspond to oxidation state of Gd in keeping with Gd^{3+} at 146.2 eV and 141 eV, respectively (**Fig. S4A**). As it is apparent in the XRD data of two different Gd_2O_3 nanoparticles (**Fig. S4B**), the peaks are quite broad as it is expected for such thin plates (< 1.2 nm).[36, 38, 40] By overlapping the reference peaks using JCPDS card, the Gd_2O_3 nanoparticles contained both cubic and monoclinic structures[38], with the larger 22 nm Gd_2O_3 nanoparticles presenting more abundantly monoclinic features.

In order to be employed as T_1 MR contrast agents, the Gd_2O_3 nanoparticles have to be transferred to water using biocompatible coatings. These are responsible for two seemingly opposite functions: preventing the release of toxic Gd^{+3}-ions[15-19], modulating for the interaction of water molecules with the surface Gd^{+3}-ions. Two different surface coating strategies were considered: a dense and thin oleic acid bilayer; an octylamine modified polyacrylic acid (PAA-OA) layer (**Fig. S5**).[29, 30, 41] In both cases, the original organic layer present at the nanoparticle interface was not disturbed. **Fig. 2(a)** illustrates the phase transfer process using oleic acid and PAA-OA. In the case of the oleic acid bilayer, a free acid group is presented at the surface. On the other hand, the PAA-OA wraps the organic amine to the particle leaving the PAA to impact stability in aqueous solutions. Note that polyacrylic acid co-polymers represent a very different kind of surface coating as compared to the OA bilayers. In fact, these amphiphilic polymers contain both hydrophobic tails (octylamine (OA)) and hydrophilic COOH groups. This derives from the fact that the hydrophobic OA surrounds the hydrophobic Gd_2O_3 nanoparticles, whereas the hydrophilic chain transfers them into water. This process does not require a direct ligand exchange of the nanoparticle surface coating, but rather encases the particles in another thicker layer of polymer. As a result, the PAA-OA polymer coated Gd_2O_3 nanoparticles tend to have a larger hydrodynamic diameter (core size 22 nm, oleic acid coating 43 nm, and PAA-OA coating 47 nm, **Fig. S6** and **Table S1**).
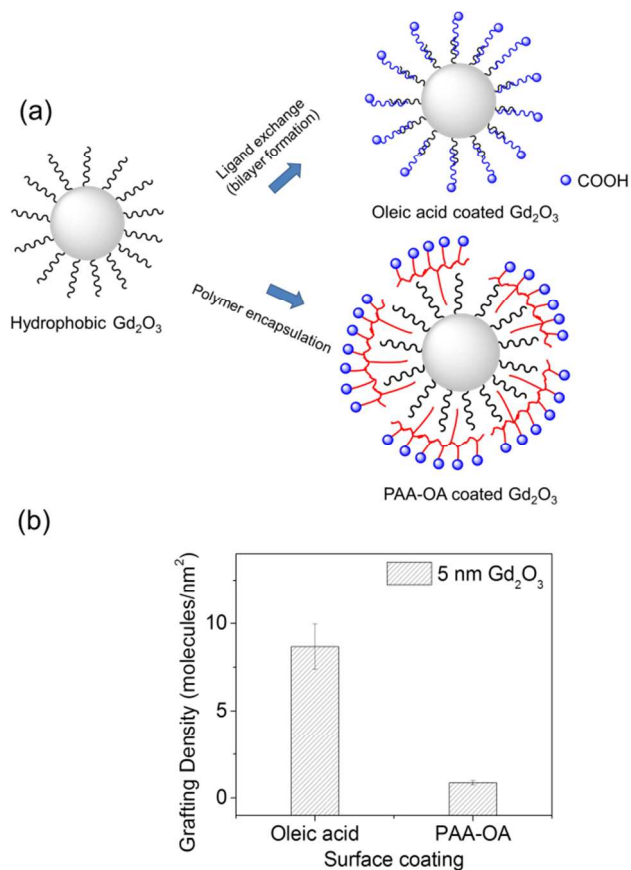
Fig. 2 Phase transfer of Gd_2O_3 nanoparticles using oleic acid bilayer and poly acrylic acid (PAA)-octylamine (OA) (PAA-OA) polymer. (a) Schematic diagram of phase transfer method of ligand exchange using oleic acid and polymer encapsulation using PAA-OA. (b) The grafting densities of oleic acid and PAA-OA by the calculation of total organic carbon (TOC) analysis (see experimental section).

Both the oleic acid and PAA-OA capped Gd_2O_3 nanoparticles had negative surface charges, with a zeta-potential value ranging from -60 to -80 mV as a function of the nanoparticle diameter. The hydrodynamic size of the coated Gd_2O_3 nanoparticles was monitored over time at various temperatures and under different buffer conditions, pH, and ionic strengths. While both coating strategies provided a good stability under most tested conditions, the PAA-OA Gd_2O_3 nanoparticles were more stable in aqueous solutions than oleic acid capped Gd_2O_3 nanoparticles (see **Fig. S7** to **Fig. S10,** and **Table S2**).

Another important feature for both nanoparticles is the surface density of the coating agent in that it would impact the access of water molecules to the superficial Gd^{3+}-ions, and thus the MRI properties of the nanoparticles. The surface polymer coverage can be determined by total organic carbon analysis (TOC).[31] Since the grafting density decreases as the molecular weight of the polymer increases, a high molecular weight polymer would have lower surface densities and offer more easy access to water molecules. The molecular weights of oleic acid and PAA-OA are 283 and 2783 g/mol, respectively.[29, 30] Using TOC, on the 5 nm Gd_2O_3 nanoparticles, the larger molecular weight coating (PAA-OA) gave a grafting density ten times smaller than that of the smaller molecular weight oleic acid coating (**Fig. 2(b)**), namely 8.67 molecules/nm² for the PAA-OA and 0.86 molecules/nm² for the oleic acid bilayer.

Relaxometric characterization of Gd$_2$O$_3$ nanoplates. Contrast agents for Magnetic Resonance Imaging (MRI) are evaluated by their relaxivity ($r_{1,2}$). The longitudinal (T_1) and transversal (T_2) relaxation times were measured for various nanoparticle suspensions using a bench top relaxometer (Bruker Minispec, 1.41 T), whereas the Gd concentrations were assessed by elemental analysis (ICP-OES). **Fig. 3 (a) and (b)** shows the r_1 and r_2 relaxivity values for both the oleic acid and PAA-OA capped Gd$_2$O$_3$ nanoparticles with a core diameter of 2 nm. The r_1 and r_2 of oleic acid capped Gd$_2$O$_3$ nanoparticles were 7.96 and 24.96 (mM·s)$^{-1}$, respectively. The r_1 and r_2 of PAA-OA capped Gd$_2$O$_3$ nanoparticles were significantly higher reaching 47.20 and 82.39 (mM·s)$^{-1}$, respectively. Specifically, the r_1 relaxivity of the 2 nm PAA-OA coated Gd$_2$O$_3$ nanoparticles is 10 times higher than that of the commercially available Gd-DTPA (mM·s)$^{-1}$, at 1.41 T (**Fig. 3(c)**).[42] Such a r_1 value is also 5 times higher than that reported for PEG coated gadolinium oxide (8.8 -9.4 (mM·s)$^{-1}$) with a 2.2 nm core[21, 22] and for the D-glucuronic acid coated gadolinium oxide (9.9 (mM·s)$^{-1}$) with a 1 nm core, at 1.41 T.[24] Such a significant enhancement in relaxivity as compared to free Gd-DTPA molecules should be ascribed to the immobilization of the Gd^{3+}-ions on the surface of the nanoplates and the modulation of the water molecule diffusion by the surface coating.[43, 44] This high relaxativity values are also confirmed by the phantom images presented in **Fig. 3(d)**. At the same concentration, T_1-weighted MR images of PAA-OA capped Gd$_2$O$_3$ nanoparticles were much brighter than oleic acid Gd$_2$O$_3$ nanoparticles and commercially available Gd-DTPA molecules, for a given Gd concentration.
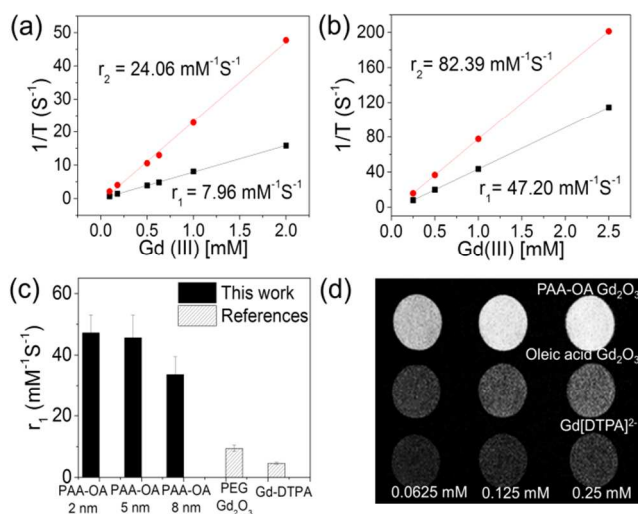
Fig. 3 Plots of the r_1 and r_2 and T_1 weighted MR images. (a) Plots of the r_1 and r_2 of oleic acid bilayer coated Gd$_2$O$_3$ nanoparticles as a function of Gd(III) ion concentration. (b) Plots of the r_1 and r_2 of PAA-OA coated Gd$_2$O$_3$ nanoparticles as a function of Gd (III) ion concentration. The r_1 and r_2 values were calculated from the slopes. The r_1 value of PAA-OA coated Gd$_2$O$_3$ nanoparticle with diameter 2 nm is 10 times higher than Gd-DTPA (4.3 mM^{-1}S^{-1}) at 1.41 T. (c) Graph of PAA-OA coated Gd$_2$O$_3$ nanoparticles (2, 5, and 8 nm) showing high r_1 relaxivity values and the reference works of Gd-DTPA[4, 5, 21, 42] and PEG Gd$_2$O$_3$[22]. (d) T_1 weighted MR images of the oleic acid coated 2 nm Gd$_2$O$_3$, PAA-OA coated 2 nm Gd$_2$O$_3$, and Gd-DTPA (magnevist) depending on their Gd (III) concentration.

The r_1 and r_2 relaxivities of the tested Gd$_2$O$_3$ nanoparticles are listed in **Table 1**. **Table 1** gives the r_1 and r_2 relaxivities and their r_1/r_2 ratio as derived from the slopes of the plot of 1/T and concentration of Gd^{3+}-ion atoms. From the data, it appears that the PAA-OA coated Gd$_2$O$_3$ nanoparticles have six to eight times higher r_1 and r_2

values as compared to the oleic acid coated Gd$_2$O$_3$ nanoparticles, for the same core diameter. The r_1/r_2 ratio of Gd$_2$O$_3$ nanoparticle is also an important factor to maximize the T_1 contrast effect.[45-47] The average r_1/r_2 ratios for the oleic acid and PAA-OA capped Gd$_2$O$_3$ nanoparticles were 0.4 and 0.6, respectively. These values are similar to those of the commercially available Gd-DTPA (0.9) and PEG gadolinium oxide nanoparticles (0.7).[24]

Table 1. r_1 and r_2 relaxivities and r_1/r_2 ratios of Gd$_2$O$_3$ nanoparticles from the slopes of the plot of 1/T and concentration of Gd ions.

Sample	Coating	Core Size (nm)	r_1 (mM^{-1} S^{-1})	r_2 (mM^{-1} S^{-1})	r_1/r_2	B_0 Field (T)
Gd-DTPA[5, 42]	-	-	4.3	4.9	0.9	1.41
Gd$_2$O$_3$[22]	PEG	3	9.4	13.4	0.7	1.41
Gd$_2$O$_3$	Oleic acid	2	8.0 ± 0.3	24.1 ± 1.4	0.3	1.41
	Oleic acid	5	6.0 ± 0.5	11.2 ± 2.3	0.5	1.41
	Oleic acid	8	5.5 ± 0.4	16.0 ± 4.3	0.3	1.41
	Oleic acid	11	4.6 ± 0.5	10.3 ± 2.2	0.4	1.41
	Oleic acid	22	3.0 ± 0.4	6.4 ± 0.2	0.5	1.41
	PAA-OA	2	47.2 ± 5.8	82.4 ± 9.9	0.6	1.41
	PAA-OA	5	45.6 ± 7.3	75.1 ± 4.4	0.6	1.41
	PAA-OA	8	33.7 ± 5.8	70.0 ± 6.5	0.5	1.41
	PAA-OA	11	32.4 ± 2.5	67.3 ± 3.5	0.5	1.41
	PAA-OA	22	21.1 ± 6.6	32.4 ± 9.6	0.7	1.41

The variation of the r_1 relaxivity with the nanoparticle core diameters can be related to the number of surface metal ions (N) interacting with the water molecules. Gd$_2$O$_3$ nanoparticles have a high surface to volume ratio, as the core diameter is smaller. In contrast with Gd-DTPA molecules (N=1), Gd$_2$O$_3$ nanoparticles concentrate a large number of Gd^{3+}-ions on the surface (N), possessing high electron spin (S= 7/2), in a small volume. All the Gd^{3+}-ions on the surface can significantly reduce the characteristic longitudinal relaxation time T_1 of the water molecules.[24] As the core diameter of Gd$_2$O$_3$ nanoparticles get smaller, the number of surface Gd^{3+}-ions in a certain volume increase. This leads to a higher relaxivity per total Gd concentration.

In 2009, the work of Lee and colleagues, and reference therein, reported on the dependence of the r_1 relaxivity with the diameters of the nanoparticles, showing that as the core diameter varies from 1.1 to 30 nm the r_1 relaxivity decreases from 9.9 to 0.1 (mM·s)$^{-1}$.[24] By tuning the size of our ultrathin gadolinium nanoplates, we confirmed that Gd$_2$O$_3$ nanoparticles (2 to 22 nm) had high r_1 relaxivity and that the r_1 values decreases as the core size increases for both oleic acid and PAA-OA coated nanoparticles (**Fig. 4**).

The r_1 relaxivities of oleic acid and PAA-OA coated Gd$_2$O$_3$ nanoparticles varied from 7.96 to 3.03 (mM·s)$^{-1}$ and 47.2 to 21.1 (mM·s)$^{-1}$, respectively, as the core diameter increased from 2 to 22 nm. Indeed, the surface to volume ratio (S/V) and number of surface gadolinium ions in the nanoplates contribute significantly to the relaxation time of the water molecules. Moreover, the surface coating of the Gd$_2$O$_3$ nanoparticles affect also the relaxivity in that it modulates the access of water molecules to the Gd^{+3}-ions. The oleic acid (small molecular weight, Mw=283 g/mol) coated Gd$_2$O$_3$ nanoparticles have much lower r_1 relaxivity values than PAA-OA (high molecular weight, Mw=2783 g/mol) coated Gd$_2$O$_3$ nanoparticles. The dense polymer coating obtained with the low molecular weight oleic acid bilayer reduces the access of water molecules to the nanoparticle surface thus limiting the overall

longitudinal relaxivity r_1. The opposite trend is instead observed with the less densely coated PAA-OA nanoparticles.
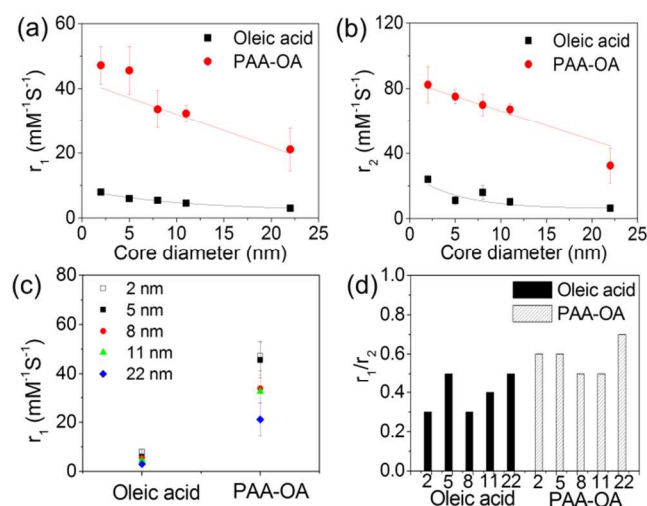
Fig. 4 Plots of r_1 and r_2 depending on the core diameters and surface coatings (a) plot of r_1 values of oleic acid bilayer and PAA-OA coated Gd_2O_3 nanoparticles as a function of the core diameters from 2 to 22 nm and (b) plot of r_2 values of oleic acid bilayer and PAA-OA coated Gd_2O_3 nanoparticles depending on the core diameters (2 to 22 nm). (c) Plot of r_1 values of different sizes of Gd_2O_3 nanoparticles depending on the coating (oleic acid bilayer and PAA-OA). (d) Plot of r_1/r_2 ratios of oleic acid bilayer and PAA-OA Gd_2O_3 nanoparticles.

The r_1 relaxivity were also measured in relevant biological media after 1 day and 4 weeks of incubation (**Fig. 5**). For most tested conditions, there was little to no change in r_1 relaxivity. The notable exceptions were for the case of phosphate buffered saline (PBS) and cell media solution (DMEM with 10 % FBS and 1 % PS). As expected, in these conditions, the r_1 relaxivity values were decreased mostly due to particle agglomeration by high ionic strength, multivalent ionic salts formation and nonspecific protein binding.[48, 49]
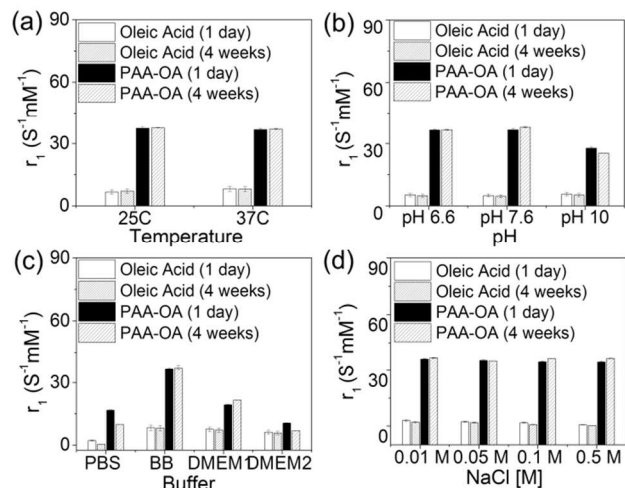
Fig. 5 Plots of r_1 relaxivity values on the different conditions including (a) temperatures (25 and 37 °C), (b) pH (6.6, 7.6, and 10), (c) buffer conditions (phosphate buffer saline (PBS), borate buffer (BB), cell media solution dulbecco's modified eagle's medium (DMEM) DMEM 1 (10 %), DMEM 2 (20 %), and (d) ionic strengths (NaCl 0.01, 0.05, 0.1, 0.5 M) after 1 day and 4 weeks.

Cytotoxicity of Gd_2O_3 nanoplates. The nanoparticles were screened in an acute *in-vitro* assay designed to evaluate whether substantial leaching of gadolinium may occur in these system and if this could affect cell viability. The existing literature suggests that Gd_2O_3 nanoparticles are relatively non-toxic.[24, 25, 27, 28, 50] For instance, Lee's group demonstrated that D-glucuronic acid coated and lanthanide doped Gd_2O_3 nanoparticles were not toxic up to 5 μM and 279 μM, respectively.[24, 28] We evaluated acute cytotoxicity using the MTS colorimetric assay with human dermal fibroblast (HDF) cells (**Fig. 6**).
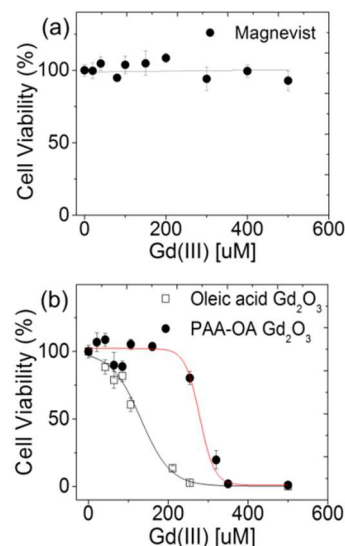
Fig. 6 *In vitro* cytotoxicity using human dermal fibroblast (HDF) cells (a) Cell viability (%) exposed to Gd-DTPA using mitochondrial activity (MTS) assay for 24 hrs. (b) Cell viability data when introduced oleic acid and PAA-OA Gd_2O_3 nanoparticles (8 nm core diameter) using MTS assay. The cells were alive up to 500 *u*M of Gd-DTPA. The LC_{50} of oleic acid and PAA-OA coated Gd_2O_3 nanoparticles were 120 uM and 270 *u*M of Gd(III), respectively.

Comparing with oleic acid coated Gd_2O_3 nanoparticles, the PAA-OA coated Gd_2O_3 nanoparticles were more stable and less toxic. From the LC_{50} value, giving the lethal dose required for half of the cells to die, the percentages of cell viability were calculated.[51, 52] The LC_{50} of oleic acid and PAA-OA coated nanoparticles were 120 μM and 270 *μ*M, respectively. This cell viability data confirmed that PAA-OA coated Gd_2O_3 nanoparticles were much less toxic than the same materials with an oleic acid coating. Note that the excellent relaxivity r_1 and low toxicity of the Gd_2O_3 nanoparticles would support their possible application as MRI contrast agents.

Conclusions

We have synthesized Gd_2O_3 nanoplates with a size ranging from 2 nm to 22 nm by fine tuning various experimental conditions, including the monomer concentration, surfactant ratio, and synthesis time. The surface of the Gd_2O_3 nanoparticles was capped either using an oleic acid bilayer or a PAA-OA polymer coating. The superior coating stability was assessed under various experimental conditions, by changing the temperature, pH, buffer, and ionic strength. From the DLS and zeta analysis, the water-soluble Gd_2O_3 nanoparticles were not aggregated and stable for more than 1 month. The longitudinal relaxivity r_1 of the 2 nm Gd_2O_3 nanoplates was

found to be up 10 times higher than that of the commercially available Gd-DTPA (~50 $(mM \cdot s)^{-1}$ vs ~4 $(mM \cdot s)^{-1}$). Via *in vitro* cell viability analysis, we have demonstrated that Gd_2O_3 nanoparticles with a PAA-OA coating have no significant cytotoxicity effect up to a Gd concentration of 250 μM. These Gd_2O_3 nanoplates represent a new class of T_1 MR contrast agents with a high relaxivity and a favorable toxicity profile.

Acknowledgements

Notes and references

[a] Department of Chemistry, Rice University, Houston, TX 77005, USA.

[b] Department of Translational Imaging and Department of Nanomedicine, The Methodist Hospital Research Institute, Houston, TX 77030, USA.

[c] Drug Discovery and Development Department, Istituto Italiano di Tecnologia, Genova 16163, Italy.

Electronic Supplementary Information (ESI) available: [The histograms of Gd_2O_3 nanoparticles ranging from 2 to 22 nm, TEM image of 22 nm gadolinium oxide with GIF mapping, size control by reaction parameter, XPS and XRD of Gd_2O_3 nanoparticles, phase transfer yields of oleic acid and PAA-OA coated Gd_2O_3 nanoparticles, hydrodynamic size and zeta potentials with table, long-term stability test at different temperature, buffer, pH, and ionic strength conditions with tables]. See DOI: 10.1039/b000000x/

References

1.   A. Fransson-Andreo, *Radiother Oncol.*, 2006, **81**, S113-S113.
2.   G. A. Macdonald and A. J. Peduto, *J. Gastroen Hepatol.*, 2000, **15**, 980-991.
3.   E. Amaro and G. J. Barker, *Brain and Cognition.*, 2006, **60**, 220-232.
4.   P. Caravan, J. J. Ellison, T. J. McMurry and R. B. Lauffer, *Chem. Rev.*, 1999, **99**, 2293-2352.
5.   R. B. Lauffer, *Chem. Rev.*, 1987, **87**, 901-927.
6.   E. J. Werner, A. Datta, C. J. Jocher and K. N. Raymond, *Angew. Chem. Int. Ed.*, 2008, **47**, 8568-8580.
7.   H. J. Weinmann, W. Ebert, B. Misselwitz and H. Schmitt-Willich, *Eur. J. Radiol.*, 2003, **46**, 33-44.
8.   S. Laurent, D. Forge, M. Port, A. Roch, C. Robic, L. V. Elst and R. N. Muller, *Chem. Rev.*, 2010, **110**, 2574-2574.
9.   S. Laurent, D. Forge, M. Port, A. Roch, C. Robic, L. V. Elst and R. N. Muller, *Chem. Rev.*, 2008, **108**, 2064-2110.
10. C. F. G. C. Geraldes and S. Laurent, *Contrast Media & Molecular Imaging*, 2009, **4**, 1-23.
11. J. W. M. Bulte and D. L. Kraitchman, *Nmr Biomed.*, 2004, **17**, 484-499.
12. S. Aime, A. Barge, C. Cabella, S. G. Crich and E. Gianolio, *Current Pharmaceutical Biotechnology*, 2004, **5**, 509-518.
13. J. W. M. Bulte, T. Douglas, B. Witwer, S. C. Zhang, E. Strable, B. K. Lewis, H. Zywicke, B. Miller, P. van Gelderen, B. M. Moskowitz, I. D. Duncan and J. A. Frank, *Nat. Biotech.*, 2001, **19**, 1141-1147.
14. C. Cabella, S. G. Crich, D. Corpillo, A. Barge, C. Ghirelli, E. Bruno, V. Lorusso, F. Uggeri and S. Aime, *Contrast Media & Molecular Imaging*, 2006, **1**, 23-29.
15. P. Marckmann, L. Skov, K. Rossen, A. Dupont, M. B. Damholt, J. G. Heaf and H. S. Thomsen, *Journal of the American Society of Nephrology*, 2006, **17**, 2359-2362.
16. T. Grobner, *Nephrol. Dial. Transpl.*, 2006, **21**, 1745-1745.
17. E. A. Sadowski, L. K. Bennett, M. R. Chan, A. L. Wentland, A. L. Garrett, R. W. Garrett and A. Djamali, *Radiology*, 2007, **243**, 148-157.
18. D. R. Broome, M. S. Girguis, P. W. Baron, A. C. Cottrell, I. Kjellin and G. A. Kirk, *Am. J. Roentgenol.*, 2007, **188**, 586-592.
19. P. H. Kuo, E. Kanal, A. K. Abu-Alfa and S. E. Cowper, *Radiology*, 2007, **242**, 647-649.
20. M. Engstrom, A. Klasson, H. Pedersen, C. Vahlberg, P. O. Kall and K. Uvdal, *Magn. Reson. Mater. Phy.*, 2006, **19**, 180-186.
21. J. L. Bridot, A. C. Faure, S. Laurent, C. Riviere, C. Billotey, B. Hiba, M. Janier, V. Josserand, J. L. Coll, L. Vander Elst, R. Muller, S. Roux, P. Perriat and O. Tillement, *J. Am. Chem. Soc.*, 2007, **129**, 5076-5084.
22. M. A. Fortin, R. M. Petoral, F. Soderlind, A. Klasson, M. Engstrom, T. Veres, P. O. Kall and K. Uvdal, *Nanotechnology*, 2007, **18**. 395501-395510.
23. M. Ahren, L. Selegard, A. Klasson, F. Soderlind, N. Abrikossova, C. Skoglund, T. Bengtsson, M. Engstrom, P. O. Kall and K. Uvdal, *Langmuir*, 2010, **26**, 5753-5762.
24. J. Y. Park, M. J. Baek, E. S. Choi, S. Woo, J. H. Kim, T. J. Kim, J. C. Jung, K. S. Chae, Y. Chang and G. H. Lee, *ACS Nano*, 2009, **3**, 3663-3669.
25. L. J. Zhou, Z. J. Gu, X. X. Liu, W. Y. Yin, G. Tian, L. Yan, S. Jin, W. L. Ren, G. M. Xing, W. Li, X. L. Chang, Z. B. Hu and Y. L. Zhao, *J. Mater. Chem.*, 2012, **22**, 966-974.
26. J. Y. Park, E. S. Choi, M. J. Baek, G. H. Lee, S. Woo and Y. Chang, *Eur. J. Inorg. Chem.*, 2009, 2477-2481.
27. L. Faucher, M. Tremblay, J. Lagueux, Y. Gossuin and M. A. Fortin, *ACS Appl. Mater. Inter.*, 2012, **4**, 4506-4515.
28. W. Xu, J. Y. Park, K. Kattel, B. A. Bony, W. C. Heo, S. Jin, J. W. Park, Y. Chang, J. Y. Do, K. S. Chae, T. J. Kim, J. A. Park, Y. W. Kwak and G. H. Lee, *New. J. Chem.*, 2012, **36**, 2361-2367.
29. A. Prakash, H. G. Zhu, C. J. Jones, D. N. Benoit, A. Z. Ellsworth, E. L. Bryant and V. L. Colvin, *ACS Nano*, 2009, **3**, 2139-2146.
30. S. S. Lee, H. G. Zhu, E. Q. Contreras, A. Prakash, H. L. Puppala and V. L. Colvin, *Chem. Mater.*, 2012, **24**, 424-432.
31. D. N. Benoit, H. G. Zhu, M. H. Lilierose, R. A. Verm, N. Ali, A. N. Morrison, J. D. Fortner, C. Ayendano and V. L. Colvin, *Anal. Chem.*, 2012, **84**, 9238-9245.
32. L. M. Bronstein, X. L. Huang, J. Retrum, A. Schmucker, M. Pink, B. D. Stein and B. Dragnea, *Chem. Mater.*, 2007, **19**, 3624-3632.
33. G. S. Chaubey, C. Barcena, N. Poudyal, C. B. Rong, J. M. Gao, S. H. Sun and J. P. Liu, *J. Am. Chem. Soc.*, 2007, **129**, 7214-7215.
34. R. Si, Y. W. Zhang, H. P. Zhou, L. D. Sun and C. H. Yan, *Chem. Mater.*, 2007, **19**, 18-27.
35. G. K. Das, B. C. Heng, S. C. Ng, T. White, J. S. C. Loo, L. D'Silva, P. Padmanabhan, K. K. Bhakoo, S. T. Selvan and T. T. Y. Tan, *Langmuir*, 2010, **26**, 8959-8965.
36. S. V. Mahajan and J. H. Dickerson, *Nanotechnology*, 2007, **18**. 325605-325611.
37. J. Paek, C. H. Lee, J. Choi, S. Y. Choi, A. Kim, J. W. Lee and K. Lee, *Crystal Growth & Design*, 2007, **7**, 1378-1380.
38. S. Seo, H. Yang and P. H. Holloway, *J. Colloid. Interf. Sci.*, 2009, **331**, 236-242.
39. H. S. Yang, H. Lee and P. H. Holloway, *Nanotechnology*, 2005, **16**, 2794-2798.
40. Y. C. Cao, *J. Am. Chem. Soc.*, 2004, **126**, 7456-7457.
41. M. A. Petruska, A. P. Bartko and V. I. Klimov, *J. Am. Chem. Soc.*, 2004, **126**, 714-715.
42. J. R. Reichenbach, T. Hacklander, T. Harth, M. Hofer, M. Rassek and U. Modder, *Eur. Radiol.*, 1997, **7**, 264-274.
43. J. S. Ananta, B. Godin, R. Sethi, X. Liu, R. E. Serda, R. Krishnamurthy, R. Muthupillai, R. D. Bolskar, L. Helm, M. Ferrari, L. J. Wilson and P. Decuzzi, *Nat. Nanotech.*, 2010, **5**, 815-821.
44. R. Sethi, J. S. Ananta, C. Karmonik, M. Zhong, S. H. Fung, X. Liu, K. Li, M. Ferrari, L. J. Wilson and P. Decuzzi, *Contrast Media Mol. Imaging*, 2012, **7**, 501-508.
45. J. Q. Wan, X. H. Jiang, H. Li and K. Z. Chen, *J. Mater. Chem.*, 2012, **22**, 13500-13505.
46. B. H. Kim, N. Lee, H. Kim, K. An, Y. I. Park, Y. Choi, K. Shin, Y. Lee, S. G. Kwon, H. B. Na, J. G. Park, T. Y. Ahn, Y. W. Kim,

W. K. Moon, S. H. Choi and T. Hyeon, *J. Am. Chem. Soc.*, 2011, **133**, 12624-12631.

47. U. I. Tromsdorf, O. T. Bruns, S. C. Salmen, U. Beisiegel and H. Weller, *Nano. Lett.*, 2009, **9**, 4434-4440.

48. M. Pavlin and V. B. Bregar, *Dig J. Nanomater. Bios.*, 2012, **7**, 1389-1400.

49. S. F. Du, K. Kendall, P. Toloueinia, Y. Mehrabadi, G. Gupta and J. Newton, *J. Nanopart. Res.*, 2012, **14**. 758.

50. B. B. Zhang, H. T. Jin, Y. Li, B. D. Chen, S. Y. Liu and D. L. Shi, *J. Mater. Chem.*, 2012, **22**, 14494-14501.

51. M. Zhang, D. Aguilera, C. Das, H. Vasquez, P. Zage, V. Gopalakrishnan and J. Wolff, *Anticancer Res.*, 2007, **27**, 35-38.

52. A. Zwart, J. H. E. Arts, W. F. Tenberge and L. M. Appelman, *Regul. Toxicol. Pharm.*, 1992, **15**, 278-290.

A table of contents (TOC)
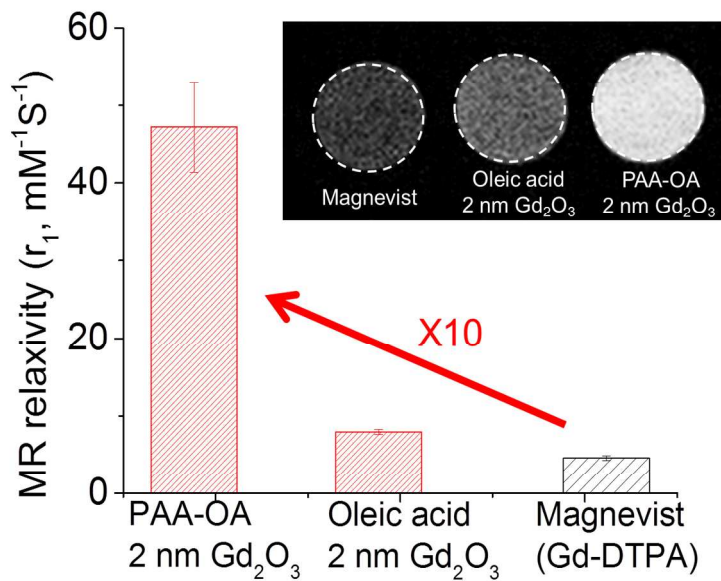
The MR relaxivity (r_1) of PAA-OA gadolinium oxide nanoplates is 10 times higher than that of FDA-approved agent.